Journal of Power Sources 491 (2021) 229576

Contents lists available at ScienceDirect

Journal of Power Sources

journal homepage: www.elsevier.com/locate/jpowsour

How to balance the voltage in serially stacked bioelectrochemical systems

Daniele Molognoni *, Pau Bosch-Jimenez, Jordi Suarez, Monica Della Pirriera, Eduard Borràs

LEITAT Technological Center, C/ de la Innovació 2, 08225, Terrassa, Spain

HIGHLIGHTS

- Stack configuration is key for a successful scale-up of BES technologies.
- Serially stacked BES can operate at higher voltages and with lower energy losses.
- Cell balance systems are required in energy-consuming, series connected BES stacks.
- An easy, passive and low-cost cell balance system based on diodes is proposed.

GRAPHICAL ABSTRACT

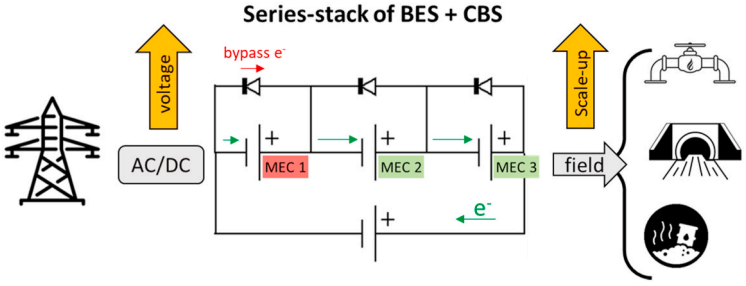

ARTICLE INFO

Keywords:
Cell balance system
Electroactive bacteria
Microbial electrolysis cell
Overvoltage
Scale-up
Stacking

ABSTRACT

Stack configuration of multiple bioelectrochemical system (BES) modules is considered nowadays as the best option for a successful scale-up of this technology, either in case of electricity-producing microbial fuel cells (MFC) or in case of electricity-consuming microbial electrolysis or electrosynthesis cells (MEC or MES, respectively). While the parallel electrical connection allows to independently operate each BES in a stack without major issues, serially stacked BES are more appealing from the point of view of energy conversion, as they suffer lower energy losses and it is possible to operate them at higher voltages. However, in the case of MEC/MES cells connected in series, high performing bioanodes can push the less-performing ones in the stack outside their "working zone", resulting in unfavorable potentials, uncontrolled voltage drops, and the temporal or permanent damage of the electroactive biofilm. A few cell balance systems (CBS) were proposed in the past but requiring expertise in power electronics. In this study an easy, passive and low-cost CBS based on commercial diodes is proposed. Three double-chamber MECs were adopted. A first set of experiments were performed to characterize the cells and understand reasons for voltage unbalance in a series-connected stack. Then, the CBS was adopted and validated.

1. Introduction

Bioelectrochemical systems (BES) result from merging electrochemical and biotechnological processes in a bioreactor. In these reactors, the oxidation and reduction reactions are spatially separated. The electrons pass through an electrical circuit in order to complete the full reaction, similarly to fuel cells and batteries [1]. However, the oxidation and/or reduction reactions in BES are catalyzed by electroactive microorganisms, which can either donate or accept electrons to/from an electrode [2,3]. In the most common applications, BES treat wastewater at the anode side, while different reduction reactions can be coupled at the cathode side. Among them, microbial fuel cells (MFC)

* Corresponding author.
E-mail address: dmolognoni@leitat.org (D. Molognoni).

https://doi.org/10.1016/j.jpowsour.2021.229576
Received 6 October 2020; Received in revised form 15 January 2021; Accepted 27 January 2021
Available online 4 February 2021
0378-7753/© 2021 The Authors. Published by Elsevier B.V. This is an open access article under the CC BY-NC-ND license (http://creativecommons.org/licenses/by-nc-nd/4.0/).

reduce oxygen to water while producing electricity, microbial electrolysis cells (MEC) produce hydrogen and microbial electrosynthesis cells (MES) generate different value-added chemicals like volatile fatty acids or alcohols [4]. A series of further acronyms are present in BES literature, relatively with specific fields of application of this flexible technological platform [5,6]. Nowadays, the most promising fields for BES application are represented by energy storage (though a power-to-gas approach), bioelectrochemically-assisted anaerobic digestion, microbial desalination, electro-bioremediation of contaminated sites, recovery of energy and/or resources from residual streams like wastewater [7–10].

However, successful scale-up of BES technology from laboratory to pilot-scale plants remains the major challenge [11,12]. A few experiences can be found in the literature, showing that the scale-up strategy should be based on a combination of stacking individual reactors and increase of reactor volume, maintaining geometric invariables like the ratio between electrode surface and reactor volume [11,13,14]. Stack configuration might be the best option either in case of electricity-producing MFCs or electricity-consuming MEC/MES. Multiple MFC cell stack designs were demonstrated in UK [15] and Ghana [16], for the treatment of urine and blackwater, respectively. From an electrical point of view, parallel or series stack configurations are possible. Connecting several BES in series adds the voltages, while one common current flows through all cells. In case several BES are connected in parallel, the voltage averages and the currents are added [17]. The parallel stack represents the easiest option for BES, allowing to control the voltage (and electrodes' potentials) and the independent operation of different modules, each one generating or draining the required amount of electricity from the stack [18,19].

Series-connected BES stacks are operated at higher voltage and lower current than parallel stacks. Lowering the operating current translates to decreased ohmic losses, i.e. lower resistance to the flow of electrons through electrodes and interconnections, and lower resistance to the flow of ions through electrolyte and membrane, where both terms are current dependent [20]. Moreover, a lower current can flow through thinner, cheaper electrical wiring, at equivalent values of delivered/consumed power [21]. On the other hand, increasing the voltage (from mV to V scale) is key for the definitive technology readiness level (TRL) progress and the industrial uptake of BES technologies [22].

Nowadays, most industrial power applications run at 24 V, while 1,8–3,3 V are the minimum standard values for low-voltage, low-power devices (e.g. smartphones). These voltages can be reached by DC/DC booster converters, in the case of single or parallel-connected MFC stacks [23,24], where such power management systems (PMS) were shown to increase the operational voltage of individual MFCs from 0,1 to 0,3 V to $>$ 3 V, with power efficiencies up to 70% [25]. In the case of electricity-consuming MEC/MES technology, reaching similar voltage values would necessarily require the series stack connection of multiple cells, which however is more delicate than the parallel alternative, as described below.

In MFCs, a large difference in voltage and a reversed cell polarity (named "voltage reversal", i.e. an anode turning to behave as a cathode, or vice versa) can occur when using the series-stack connection [17,26], as a result of a non-spontaneous anode overpotential in a unit cell having a lower anode kinetics compared to the other cells [27]. In order to eliminate voltage reversal in MFCs, various control methods were suggested [28], based on: (*i*) applying a threshold resistance [29]; (*ii*) supporting an assistance current [30]; (*iii*) manipulating the internal resistance [31]; (*iv*) increasing the current capacity [32] and (*v*) combining electronic circuits [33].

On the other hand, in series-connected stacks of MEC/MES cells, high performing bioanodes (with good electrogenic activity) can push the less-performing ones in the stack outside their "comfort zone", i.e. forcing these weak anodes to increase their electrochemical potential, to be able to sustain the stack current [17]. Unfavorably high anode potentials, maintained in time during the start-up and/or continuous operation of the stack, can potentially lead to water electrolysis or microbial cell lysis, with consequent biofilm damage in the low-performing BES [21]. The voltage unbalance arising between the individual BES cells of the stack is likely to happen whenever wastewater feeding or recirculation conditions are uneven distributed (e.g. due to blockages of pipes), resulting in the "fuel starvation" phenomena, as named by Oh and Logan [26]. Engineering methods to balance the individual voltage drops in a series-stack of MEC/MES cells are needed, but related scientific literature is poor. Although such control electronics are commonly applied in abiotic electrochemical systems (e.g. electrical batteries) [34], only one previous study was performed relatively to BES field, to authors' knowledge. An active cell balance system (CBS), controlling individual MECs electrically connected in series, was based on metal oxide semi-conductor field-effect transistors (MOSFET) switches, as the central mechanism to dynamically adapt the power input to the performance variation of bioanodes [21]. However, the development and application of such a control system required some experience in power electronics and might not have been well understood by the general BES practitioner (mostly electrochemists or environmental engineers), this likely being one of the reasons why almost no scientific literature exists about series-stacked BES.

In this study, an easily imposed, low-cost, and passive CBS solution for a series-connected stack of MECs was proposed, based on commercial diodes. Three double-chamber MEC reactors were adopted at the purpose. The diodes were placed in parallel to each MEC in the series-stack, and they acted as a passive "bypass line", allowing the excess current to flow outside of the individual cell when its voltage drop exceeded the disruptive voltage of the diode. The diodes were selected for their disruptive voltage to be slightly lower than the maximum voltage tolerated by the individual MEC in the stack. This way, when one of the cells in the stack underperformed, and its voltage increased over the disruptive voltage of the diode, part of the current flowed through the diode itself, bypassing the cell and avoiding biofilm damage at the anode. A first set of experiments were performed to characterize the MEC cells and understand the reasons for voltage unbalance, in a serially-connected stack. Then, the CBS was adopted and validated, in different operation scenarios.

2. Materials & methods

Three double-chamber, H-type MEC reactors were adopted for the experiments. Each MEC chamber was made out of pirex glass bottle with a side arm tube, having a liquid volume of 300 mL (VidraFoc, Spain). The two chambers were separated through a cationic exchange membrane (CMI-7000, Membrane International, USA) of 12,6 cm^2 surface, which was clamped between the two side arm tubes, similarly to the setup reported in Ref. [35]. The total length of the two connected tubes was of 9 cm. The anode was a carbon fibers brush, with diameter of 2,5 cm and length of 2,5 cm, provided with an internal current collector in Ti (Mill-Rose, USA). The projected cylinder surface of the brush was of 29 cm^2, while fibers total area was estimated (based on their geometrical characteristics) to be approx. 2300 cm^2. The cathode was based on a Ti mesh covered with 12 g/m^2 Ir-MMO (Magneto, The Netherlands), as catalyst for the hydrogen evolution reaction (HER) [36]. Anode and cathode were placed in the middle of the respective bottle chambers, facing each other, at a distance of 11 cm. An Ag/AgCl reference electrode (+0195 V vs SHE, Xi'an Yima Opto-electrical Technology, China) was placed in the anode chamber of each MEC, outside the electric field, at ≈1,5 cm from the anode [37]. The 3 double-chamber MECs were placed on a 6-position magnetic stirrer (MixDrive 6HT, 2mag, Germany), applying a stirring rate of 140 rpm. Anode and cathode chambers of each MEC were maintained at atmospheric pressure by inserting a needle with a 0,22 μm filter to the cap. In case of the cathode chambers, the produced H_2 was collected into Tedlar bags, with the only purpose not to disperse it into the environment. A photo of the experimental setup is provided as Supplemental Information, hereafter SI (Figure S1).

The anodes were first inoculated in chronoamperometric mode, at progressively lower potentials (from −0,1 to −0,35 V vs Ag/AgCl), within single-chamber BES cells adopting a gas diffusion layer catalyzed with MnO_2 as air-cathode (SGL, Germany). A potentiostat (VMP3, Bio-Logic, France) was adopted for the electrochemically controlled operation. The cells were fed in batch mode by a mixture of 50% acetate-based mineral medium [22] and 50% wastewater effluent from a previously operated, laboratory scale MFC [38].

After inoculation, the anode chambers were coupled with the cathode chambers and operated like H_2-producing MECs in batch mode, feeding them with 30 mM acetate-based medium as anolyte, and 100 mM phosphate buffer solution (PBS) as catholyte (media characteristics in Table 1). The electrochemical operation conditions are described in section 2.2.

2.1. Polarization curves and diodes selection

The MECs were electrochemically characterized using the potentiostat, through a polarization curve, performed by sequential chronoamperometric steps of 30 min duration (and 0,1 V amplitude) at different anode potentials, ranging from open circuit (near −0,55 V vs Ag/AgCl) up to +0,2 V vs Ag/AgCl.

In a view of series-stack application of MECs, commercial diodes (ref. STTH2R06, ST Microelectronics, USA, maximum forward current of 2 A, maximum forward voltage drop of 1,7 V) were selected and combined, in a way that their disruptive voltage was slightly lower (i.e. few hundreds of mV) than the maximum voltage tolerated by the individual MECs in the stack.

2.2. MECs operation and characterization

The cells were fed in batch mode. At the beginning of each batch, the pH of the two electrolytes was equal. Once the batch cycle was closed, both anode and cathode chamber were emptied and rinsed with water, and the respective electrolyte solutions were replaced by fresh ones (to avoid voltage loss due to pH gradient). Batch tests of individual MECs were initially performed, in chronopotentiometric mode applying a constant current near to the optimal operation point determined by polarization curves (9 mA). This way, the evolution of anode and cathode potentials along a batch cycle could be determined, in comparison with the reference electrode. The anode potential of each MEC was limited (not poised) through the potentiostat to +0,2 V vs Ag/AgCl to prevent electroactive biofilm from damage. In other terms, the anode potential was let free to vary along the batch cycle, until reaching the threshold value, when the experiment was automatically stopped by the potentiostat.

Then, several batch tests were performed by series-connecting the 3 MECs through the potentiostat, operating them in chronoamperometric mode at different values of stack voltage (3; 3,5; 4 and 4,5 V). Once cell voltage unbalance occurred, the position of the cells in the stack was switched, to determine its eventual effect on voltage distribution. After the first series-stack trial, the voltage drop of each individual MEC in the stack was limited to 1,8 V, to protect the anode biofilm. Then, the stack was operated at progressively increasing voltage values, until one of the cells experienced this threshold voltage drop, due to voltage unbalance, reaching what can be named as the “breakpoint” of the stack.

After each batch cycle was ended due to stack breakpoint, a transitional operation was performed for each individual MEC. This consisted in applying a constant anode potential of −0,35 V vs Ag/AgCl, until optimal performance of electroactive biofilm was recovered. Once current generation of the 3 MECs was stable, this transitional technique was stopped, and the cells were assembled again in series-stack configuration.

As a last experiment, the diodes composing the CBS were installed in parallel to each MEC, and batch tests were repeated with the protected stack, at a constant stack voltage of 4,5 V (chronoamperometric mode). Besides, the stack was also tested in chronopotentiometric mode, at 9 mA. Electrical efficiency of the proposed CBS was calculated and compared, with the two operation modes.

Table 1
Physical-chemical characteristics of the media adopted for MECs feeding.

Medium	pH (−)	Conductivity (mS/cm)	COD (g/L)
Anolyte	7,5	10,3	1,95
Catholyte	7,5	14,4	–

2.3. Analysis and calculations

During the initial tests with the individually operated MECs, two electrolyte samples per day were collected from the anode and cathode chambers. The samples were analyzed in terms of pH and conductivity (HQ40 multimeter, Hach Lange, Spain). The soluble part of the chemical oxygen demand (COD) was also determined for the anolyte samples (LCK 514 kits, Hach Lange, Spain). The rate of COD consumption in the anode chamber of the 3 MECs was evaluated through a regression analysis, by calculating the first order kinetic constant (k) and the correlation coefficient (R^2).

During the tests with the series-connected stack, samples of anolyte and catholyte were punctually collected, with a special focus to the stack breakpoint, to determine the reasons for voltage unbalance among the cells.

The CBS power efficiency (η_{power}), for a series-connected stack of BES, was calculated by eq. (1).

$$\eta_{power} = 1 - \frac{P_{diode}}{P_{stack}} = 1 - \frac{\sum_i ((V)_i I_{diode_i})}{(V)I} \quad [1]$$

In the equation, P_{diode} represents the electrical power consumed by the CBS (i.e. power wasted through bypass diodes), while P_{stack} represents the total power consumed by the stack of BES. The voltage applied to the BES stack is represented by ΔV while I is the consumed current. The term ΔV_i refers to the voltage drop of the i-th cell. The bypass current, flowing through the i-th diode ($Idiode_i$), was calculated based on ΔV_i, through the diode characteristic curve (eq. (2)).

3. Results and discussion

The polarization curves of the 3 MECs were performed with fresh anolyte and catholyte, after reaching a stable cell operation (Fig. 1). The potentiostat needed 4 h to complete each polarization curve, time during which the pHs of anolyte and catholyte did not vary significantly.

Analyzing the curves in Fig. 1 A, it appears that current consumption of MECs evolved linearly with the applied voltage up to a “saturation point”, where substrate diffusion limitation, pH gradient over the membrane, or other physical-chemical factors led to an unstable and decreasing trend of the electrical current. Fig. 1 B shows that the kinetics of the bioanodes got limited at a potential near to −0,2 V vs Ag/AgCl. MEC 2 exhibited a significantly higher electricity production, reaching a 30% higher electrical current then the other two cells in the polarization curve. It must be noted that such a difference, although unexpected in a series of 3 replicate MECs, represented a good opportunity to show the effects of voltage unbalance in a series-connected stack of MECs and to test the proposed CBS solution.

In a view of serially stacking the 3 MECs, the saturation point of the lower performing cells (MECs 1 and 3) was considered (corresponding to ≈1,4 V). The disruptive voltage of the diode (or line of diodes) to adopt for the CBS should have been the nearer as possible to this value. Fig. 2 shows the characteristic intensity-voltage curve (IV) of the diode STTH2R06 (ST Microelectronics, USA), selected for this experiment, together with the IV curves of a line of two and three diodes in series. The latter option (3 diodes in series) was the one allowing the disruptive voltage closer to the specific requirement of MECs (≈1,2 V, 200 mV

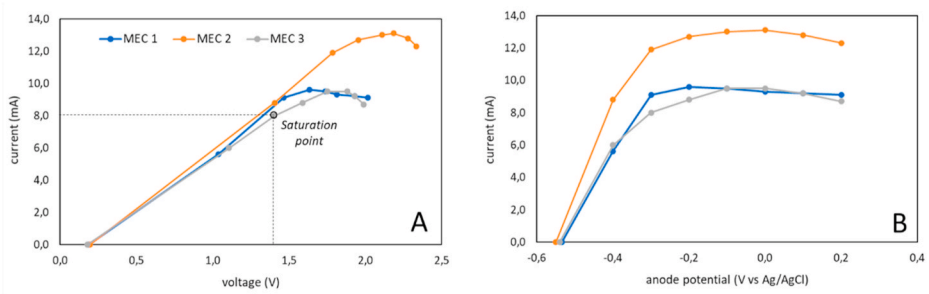

Fig. 1. Polarization curves of the 3 individual MECs. Consumed electrical current is reported versus (A) applied voltage and (B) anode potential. Saturation point of the lower performing cell (MEC 3) is identified in sub-figure A.

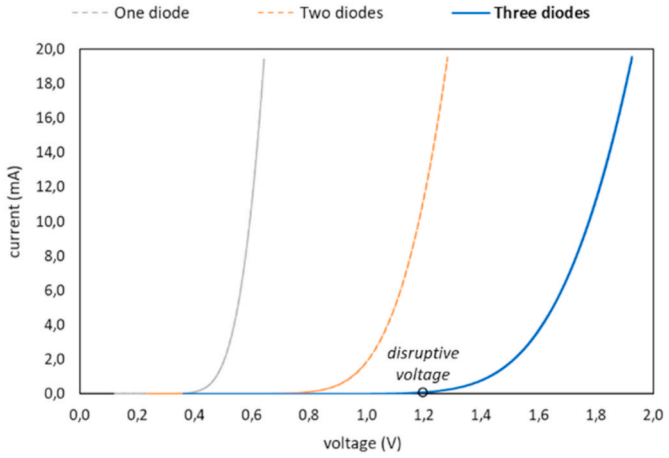

Fig. 2. Characteristic IV curves of the adopted diodes. Single diode, 2 diodes and 3 diodes in series were tested.

difference), i.e. the diode was not conducting up to a voltage of 1,2 V.

With the diodes installed in parallel to the stack of MECs, every time that one of the cells would start to underperform (its voltage drop exceeding the disruptive voltage of the diode), part of the current would flow through the diode itself, bypassing the cell. The bypass current of the i-th cell ($Idiode_i$) could be calculated through its voltage drop (ΔV_i), using the regression equation of the IV curve (eq. (2)).

$$I_{diode\,i} = 5,6345 \cdot V_i^5 - 14,387 \cdot V_i^4 + 8,5657 \cdot V_i^3 + 4,4955 \cdot V_i^2 - 5,5909 \cdot V_i + 1,2926 \quad [2]$$

This way, it was possible to evaluate the current distribution within MECs and bypass diodes, during the subsequent experiments. Also, eq. (2) was necessary to determine the CBS power efficiency, through eq. (1).

3.1. Individual MECs characterization

While polarization curves were performed in (quasi) steady-state and optimal conditions, the batch-fed MECs presented variable conditions of pH, conductivity, and COD (of anolyte) during time. While the pH and COD of the anolyte decreased during the batch duration, due to acetate oxidation reaction, the pH of the catholyte increased, due to protons reduction to H_2 and consequent accumulation of OH^-.

The kinetic constants of COD consumption were calculated for the 3 replicate MECs. The MEC 2 was far more efficient in removing COD ($k_2 = 0,33\ d^{-1}$, $R^2 = 0,94$) compared with MECs 1 and 3 ($k_1 = 0,16\ d^{-1}$ and $R^2 = 0,97$, $k_3 = 0,15\ d^{-1}$ and $R^2 = 0,97$, respectively). This explains also why MEC 2 reached a higher electrical current during the polarization curve (Fig. 1). Figure S2 (SI) shows the trends of pH and COD in the anode and cathode chambers of the three MECs during a standard batch cycle, performed at a constant current of 9 mA.

This evolution of pH and COD caused the increase of MEC overpotentials and measured voltage during the batch test, as shown by Fig. 3 A. However, the increase of overpotentials was neither linear in time nor proportional between anode and cathode electrodes. Indeed, the anode potential exhibited an abrupt increase after 2,5 days of test (Fig. 3 B), rapidly reaching a value of +0,2 V vs Ag/AgCl (safety threshold imposed through the potentiostat), corresponding to a cell voltage higher than 2,0 V. The cathode potential decreased in time following a more linear trend, likely because the reaction hereby taking place was abiotic.

The same electrochemical behavior of anode and cathode potentials might happen in a series-connected stack of MECs, whenever one of the cells reaches limiting conditions of COD or an unsustainable pH difference between anolyte and catholyte.

3.2. Series-connected stack of MECs

Fig. 4 (A-D) shows the evolution of the individual voltage drops and consumed electrical current of the 3 series-connected MECs, at different values of stack voltage (3; 3,5; 4 and 4,5 V). The individual voltage drops of the 3 MECs were well balanced during the first steps, up to a stack voltage of 4 V, while current consumption coherently increased, although slightly less than the initial indications provided by the polarization curves (Fig. 1 A). It must be remembered that the current, in a conventional series-stack, is equal to the maximum current of the least performing cell [21], which is the cell experiencing the highest overpotential (MEC 1 in Fig. 4). The potentials measured at the bioanodes remained in a "safe" range up to a stack voltage of 4 V, stabilizing on values between −0,4 and −0,2 V vs Ag/AgCl, as shown by Table 2.

At a stack voltage of 4,5 V, MEC 1 started to suffer an unbalanced voltage drop of 2 V, increasing its anode potential to unsustainable values higher than +0,2 V vs Ag/AgCl (Table 2). The current consumption decreased from 7 to 6 mA, revealing a negative effect on the electroactive biofilm. In order to avoid a similar situation, potentially leading to water electrolysis, microbial cell lysis or other undesired reactions, a threshold voltage drop of 1,8 V was imposed for each individual MEC in the stack, for the rest of the experiments, through the potentiostat software.

It must be noted that the stack voltage of 4,5 V was more than 3 times higher than the saturation value previously determined by the polarization curves (Vsat, equal to 1,4 V), inferring that in a series-connected stack of n MECs, the total applied voltage should not exceed $n \cdot$ Vsat in order for the individual voltage drops to remain balanced.

On the other hand, MEC 2 showed the lower and most stable voltage drop in the stack, at the different tested voltages. The reason lies in the fact that MEC 2 represented the best performing cell, accepting the highest current per equal value of voltage drop (see polarization curves in Fig. 1), and therefore allowing the lowest overpotentials, as long as operating at a non-limiting substrate concentration.

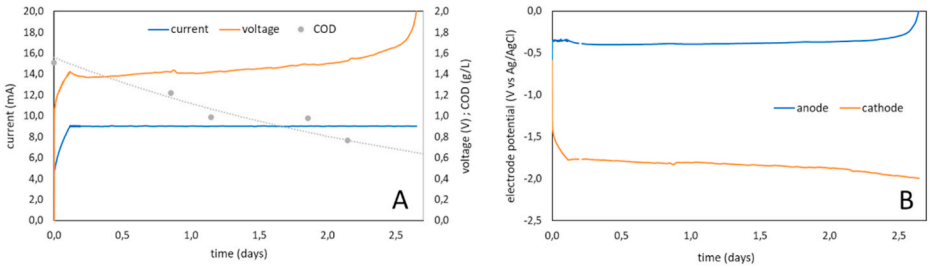

Fig. 3. Evolution of (A) applied voltage and COD, and (B) anode and cathode potential of MEC 2, during a batch cycle at constant current (9 mA). During the first 3 h of batch, the anode was polarized at −0,350 V vs Ag/AgCl.

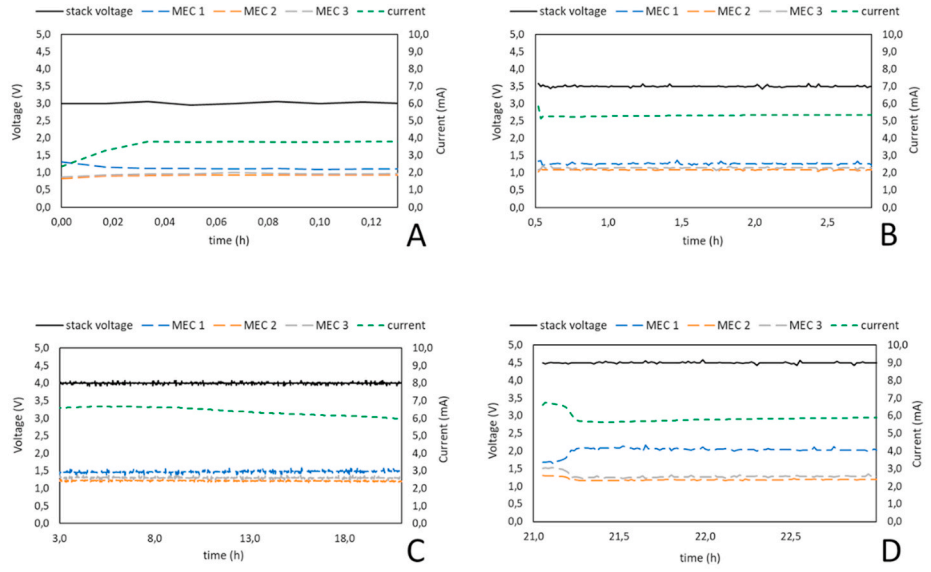

Fig. 4. Evolution of the voltage drops and consumed electrical current of 3 series-connected MECs (order: MEC1/MEC2/MEC3), at different values of stack voltage (A = 3 V; B = 3,5 V; C = 4 V; D = 4,5 V).

Table 2
Potentials of anode and cathode (E_{an} and E_{cat}, values in V vs Ag/AgCl) and cell voltage drops (ΔE, values in V) measured with the series-connected stack of MECs, at different values of stack voltage. Tue stack current (mA) measured at the end of each voltage step is also reported.

Stack voltage	Stack current	MEC 1			MEC 2			MEC 3		
		E_{an}	E_{cat}	ΔE	E_{an}	E_{cat}	ΔE	E_{an}	E_{cat}	ΔE
3,0	3,8	−0,30	−1,40	1,10	−0,45	−1,40	0,95	−0,40	−1,40	1,00
3,5	5,4	−0,31	−1,57	1,26	−0,43	−1,51	1,08	−0,37	−1,51	1,14
4,0	6,0	−0,26	−1,75	1,49	−0,40	−1,59	1,19	−0,30	−1,59	1,29
4,5	5,9	+0,26	−1,74	2,00	−0,40	−1,59	1,19	−0,31	−1,59	1,28

At this point, it was interesting to determine if MECs position in the stack could affect their individual voltage drop. For this reason, the order of cells was switched from MEC1/MEC2/MEC3 to MEC2/MEC3/MEC1, while maintaining a stack voltage of 4,5 V. The MEC 1 continued experiencing an unbalanced voltage drop of 2 V, i.e. the cell position in the stack did not affect its voltage drop (Figure S3, SI). The reasons of voltage unbalance must therefore be related with the internal conditions of the electrolytes (COD, pH and/or conductivity, among other factors).

Fig. 4 and Figure S3 refer to (quasi) steady-state operation of the stack of MECs, i.e. no substrate limitation, no significant pH gradient between anolyte and catholyte. Fig. 5 shows a different kind of experiment, where the stack of MECs was operated at increasing voltage values (from 2,5 to 3,5 V) and pushed to the breakpoint, i.e. moment when the voltage drop of the less performing MEC drifted up to 1,5 V (last measured value, before reaching the imposed threshold of 1,8 V). The voltage unbalance caused an abrupt decrease of the current from 5 to 3,5 mA. The automatic stop of the experiment avoided reaching permanent biofilm damage and allowed to continue with the experiment. However, the control system offered by the potentiostat would not be possible if operating the stack with an ordinary power source. This is the reason why to develop and test alternative control systems for real-world application.

Electrolytes were sampled and analyzed after the automatic stop of the experiment. Anolytes' pHs were near neutrality (7,13 ± 0,15) while catholytes' ones were basic (10,99 ± 0,02), for the three MECs. Interestingly, the anolyte COD of MEC 2 was lower than detection limit (<10 mg/L), while those of MECs 1 and 3 were still higher than 1000 mg/L. This observation was coherent with the higher kinetic constant for COD removal, previously determined for MEC 2 (Figure S2, SI) and demonstrated that the voltage unbalance was caused by a substrate limitation in the cell experiencing the higher voltage drop.

After this series-stack test, possibly harmful for electroactive

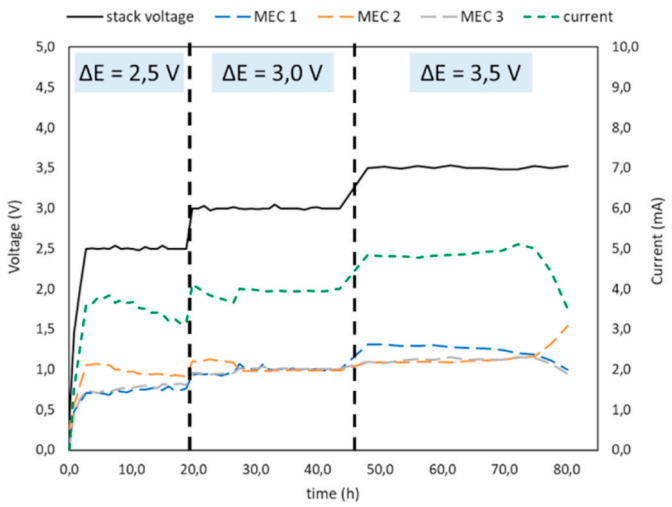

Fig. 5. Evolution of the voltage drops and consumed electrical current of 3 series-connected MECs, at different values of stack voltage, until reaching the breakpoint of the stack.

bacteria, the 3 MECs were separated and independently operated for some hours, performing an anodic CV and a chronoamperometry test, with which to verify that the bioanodes were not compromised. The typical "S-shape" of the CVs and the values of current achieved in chronoamperometry demonstrated that no permanent damage was caused to the bioanodes (Figure S4, SI). Therefore, a second test was conducted with the series-connected stack of MECs, this time reaching a stack voltage of 4 V before experiencing the breakpoint, again on MEC 2 (Figure S5, SI). After the automatic stop, the anolyte COD of MEC 2 was lower than 20 mg/L, while those of MECs 1 and 3 were of 1040 and 860 mg/L, respectively, confirming that the cell voltage unbalance was caused by a substrate limitation on MEC 2.

3.3. Proposed cell balance system (CBS)

Once verified the reason leading to voltage unbalance in a series-connected stack of BES, the selected "bypass diodes" composing the CBS were installed in parallel to each MEC, as shown in Fig. 6. The CBS purpose was to balance the individual voltage drops of MECs, independently of their internal conditions, while preventing the low-performing cells from limiting the current through the whole stack. The same tests performed without the CBS (section 3.2), at different stack voltages, were repeated for this new configuration. The results are

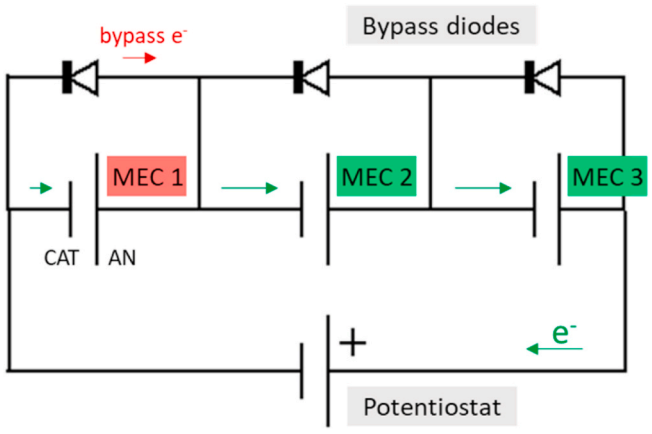

Fig. 6. Application of the CBS to the stack of MECs. Example of operation, with MEC 1 representing a low-performing cell. Part of the electrons flow through the bypass diode of MEC 1, thus maintaining the voltage balance in the stack.

resumed in Table 3 and Figure S6 (SI).

Figure S6 clearly shows that the CBS was effective in balancing the voltage drops of MECs, without risks of material damage at the anodes, also at stack voltages higher than the threshold value of 3 Vsat (last step at 4,5 V). Table 3 confirms that bioanodes were always operating at a "safe" potential, between −0,5 and −0,4 V vs Ag/AgCl, independently of the applied voltage. On the other hand, the potential of the abiotic cathode was varying from −1,4 to −1,9 V vs Ag/AgCl, to sustain the gradually increasing current of the stack. Therefore, each cell in the stack acted as an independent unit, draining the optimal amount of current from the potentiostat.

However, the CBS effectiveness in balancing the voltage came with a drawback, as MEC voltage drops higher than the disruptive voltage of the diodes allowed part of the current to bypass the cell, getting wasted as heat (Fig. 7). This situation started taking place at a stack voltage of 4 V. While at this voltage only 7% of the electrical power was lost, at 4,5 V the power loss was higher (18%), revealing the limitations of this passive control system, when not correctly applied.

The distribution of current within cell and diode was different for the 3 MECs (Fig. 7C and D), the bypass current being higher for MEC 3 in comparison with MECs 1 and 2. This because MEC 3 was the lowest performing cell, in this particular case (see Fig. 1). A previous test, shown in Figure S3 (SI), demonstrated that cell position in the stack does not affect its voltage drop, and consequently neither its current consumption.

Also in this case, Fig. 7 and Figure S6 refer to (quasi) steady-state operation of the stack of MECs. However, it was interesting to continue the test to the (eventual) stack breakpoint, in order to evaluate CBS effectiveness and efficiency along a complete batch cycle (Fig. 8).

The proposed CBS demonstrated to be effective along the whole batch cycle: the individual voltage drops of the series-connected MECs never exceeded the safety threshold of 1,8 V (indeed, the potentiostat could be replaced by a simple power source, achieving same results). The electrical current initially remained stable near 11 mA. After 24 h, it started decreasing more sharply, reaching 4,7 mA after 70 h of batch. At this point, the cell voltage drops were of 1,29, 1,63 and 1,58 V for MECs 1, 2 and 3, respectively. Same time, the diodes installed in parallel to MECs 2 and 3 were conducting 97% and 69% of the stack current, respectively, while the diode of MEC 1 was almost inactive. In other terms, most of the current was flowing outside MECs 2 and 3, lowering the CBS power efficiency to values near 40%. Physical-chemical analysis of the electrolytes confirmed the previous deduction: while anolytes of MEC 2 and 3 were "exhausted" (COD lower than 20 mg/L), that of MEC 1 still contained some oxidizable substrate (COD of 460 mg/L). The pHs of anolytes and catholytes were of 6,60 ± 0,29 and 11,56 ± 0,20, for the three MECs.

The experiment was repeated for a second time, after the transitional period at constant anode potential, but this time applying a stack voltage of 4 V. Results were similar in terms of voltage balance (see Figure S7, SI), although the CBS power efficiency remained on higher values (>90%) for the first 56 h of the batch cycle, due to the lower activation state of the bypass diodes. As previously observed, the first cell reaching a substrate limiting condition was MEC 2 (COD <50 mg/L after 68 h). At the end of the batch cycle, the cell voltage drops accounted for 1,32, 1,57 and 1,14 V for MECs 1, 2 and 3, respectively. The pHs of anolytes and catholytes were of 6,66 ± 0,24 and 11,50 ± 0,05, for the three MECs.

A final experiment was performed in chronopotentiometric mode, applying a constant current of 9 mA to the series-connected stack, protected by the CBS (Figure S8, SI). The stack remained well balanced for the first 47 h of the batch cycle, while the CBS power efficiency remained on high values (>85%). At this point, the MEC 2 started experiencing substrate limitation and a higher voltage drop, reaching 1,71 V after 68 h (at the same time, COD < 20 mg/L). Coherently, its bypass diode got activated and part of the current flowed outside of the cell, maintaining the target of 9 mA but lowering the CBS efficiency

Table 3
Potentials of anode and cathode (E_{an} and E_{cat}, values in V vs Ag/AgCl) and cell voltage drops (ΔE, values in V) measured with the series-connected stack of MECs, at different values of stack voltage, when adopting proposed CBS. The stack current (mA) measured at the end of each voltage step is also reported.

Stack voltage	Stack current	MEC 1			MEC 2			MEC 3		
		E_{an}	E_{cat}	ΔE	E_{an}	E_{cat}	ΔE	E_{an}	E_{cat}	ΔE
3,0	4,2	−0,41	−1,40	0,99	−0,46	−1,43	0,97	−0,44	−1,44	1,00
3,5	6,0	−0,43	−1,55	1,12	−0,45	−1,58	1,13	−0,43	−1,59	1,16
4,0	7,9	−0,41	−1,68	1,27	−0,42	−1,71	1,29	−0,41	−1,72	1,31
4,5	11,1	−0,39	−1,84	1,45	−0,40	−1,87	1,47	−0,38	−1,87	1,49

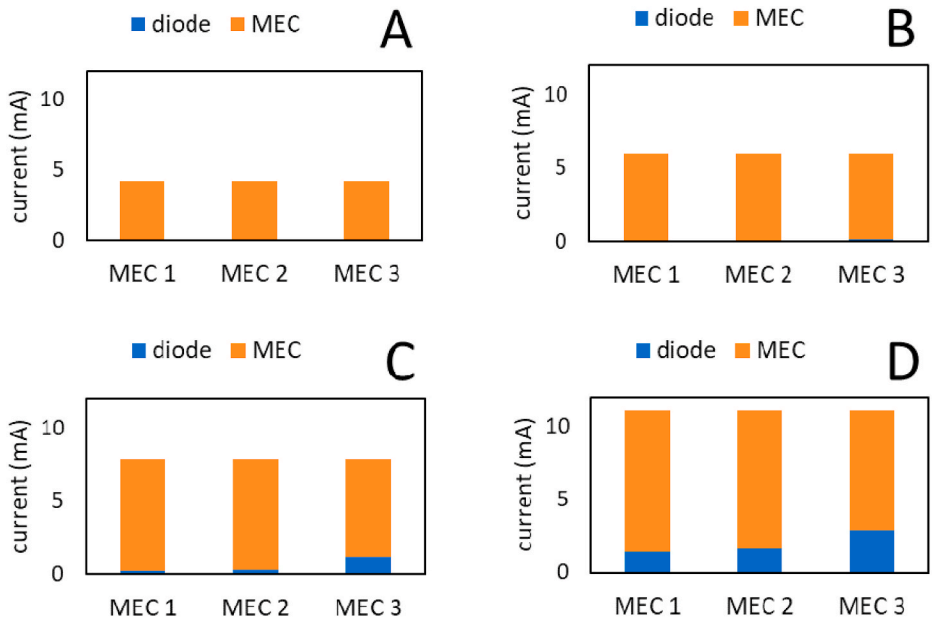

Fig. 7. Distribution of electrical current within MEC cells and bypass diodes, at different values of stack voltage (A = 3 V; B = 3,5 V; C = 4 V; D = 4,5 V).

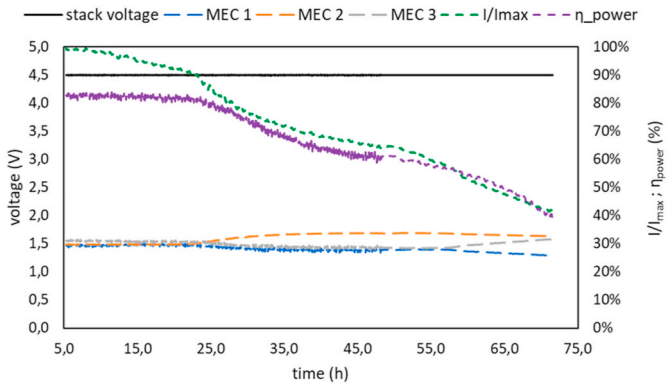

Fig. 8. Evolution of the voltage drops, consumed electrical current and CBS efficiency (normalized values) of the 3 series-connected MECs, at a stack voltage of 4,5 V, when adopting the proposed CBS.

down to 55%.

This condition looked "acceptable" in terms of cell voltage balance, but it was not electrochemically sustainable, as demonstrated by the anode potential reached by MEC 2 at the end of the cycle (Table 4). Indeed, maintaining a constant current when the substrate of an individual cell of the stack gets depleted causes a distortion of its electrodes' potentials, and the eventual onset of unwanted reactions like water electrolysis.

In resume, the CBS allowed to independently operate the three MECs composing the series-stack, each one draining the optimal/available amount of current from the substrate, while bypassing the excess one through the diodes line. The CBS worked properly with the stack operated in chronoamperometric mode (i.e. fixing the stack voltage) but may not be appropriate in chronopotentiometric operation (i.e. fixing the current), whenever the substrate is not correctly distributed/replaced within the individual MECs of the stack. The power efficiency of the proposed CBS is strictly linked with the diodes selected for the bypass line, and the applied stack voltage. By correctly setting up these two parameters, it is possible to reach high power efficiencies (>90%), comparable with those of competitor, active control systems.

It is worth mentioning that this experiment was performed in batch

Table 4
Potentials of anode and cathode (E_{an} and E_{cat}, values in V vs Ag/AgCl) and cell voltage drops (ΔE, values in V) measured with the series-connected stack of MECs in chronopotentiometric mode (stack current of 9 mA), at the end of the batch cycle.

Stack voltage	Stack current	MEC 1			MEC 2			MEC 3		
		E_{an}	E_{cat}	ΔE	E_{an}	E_{cat}	ΔE	E_{an}	E_{cat}	ΔE
4,67	9,0	−0,30	−1,79	1,49	+0,64	−1,07	1,71	−0,34	−1,81	1,47

conditions with a synthetic medium, but similar conclusions could be reached for continuously fed BES stacks, and/or real wastewater feed. In that hypothetical case, the best scenario would be to hydraulically connect all the cells in parallel, for a uniform substrate distribution, while maintaining a low hydraulic retention time, guaranteeing that none of them would reach substrate limiting conditions. Continuously providing fresh medium to the anodes, could help maintaining a balanced voltage drop within the stack of MECs, limiting the excess current flowing through the bypass diodes and finally increasing the power efficiency of proposed CBS. However, the long-term stack operation could cause a progressive fouling of the membrane(s), which most visible effect would be an increase of the internal resistance of individual MECs, i.e. a lower electrical current, per determined applied voltage [39]. It is not obvious, with the data obtained in the present study, that membrane fouling would also cause a decrease of the saturation voltage, and therefore would require a replacement of CBS diodes. However, a reduction of the CBS power efficiency in time is likely to happen. Certainly, this phenomenon must be investigated in subsequent investigation.

On the other hand, feeding the stack with a real wastewater would represent a completely different scenario (due to changes in electrolytes pH, conductivity, COD, buffer capacity, etc.). The diodes composing the CBS system, and the maximum appliable stack voltage, should be fit on purpose. The technological solution presented in this study represents a reference guide, with which to select the right parameters.

The development of this CBS solution paves the way to implement series-connected stacks of multiple BES cells, reaching high voltage levels (24 V) suitable for industrial power converters. When one of the cells would start to underperform, it could be adjusted or replaced without affecting the other cells in the stack, as the electrical current would be flowing through the bypass line. The CBS solution can be utilized for a vast number of BES technologies, especially energy storage, electro-fermentation, and electro-bioremediation (among others). The CBS allows to increase the applied voltage requirements, with concomitant increase in power density and process yield.

4. Conclusions

In this study, an easy and low-cost cell balance system (CBS), based on commercial diodes, was proposed for the first time for serially-connected stacks of electricity-consuming BES, like MEC or MES cells. The proposed CBS represented a passive alternative to the active control system previously developed by Andersen et al., in 2013 [21]. Three double-chamber MECs were batch operated in different electrochemical conditions to: (*i*) understand the reasons for cell voltage unbalance in a series-connected stack; and (*ii*) test and validate the CBS. A first set of experiments allowed to demonstrate that voltage unbalance phenomena in series-stack of MECs are caused by a substrate limitation in the cell(s) experiencing the higher voltage drop(s). Applying the CBS allowed to independently operate the three MECs composing the stack, each one draining the optimal/available amount of current from the substrate, while bypassing the excess one through the diodes line. The CBS worked properly with the stack operated in chronoamperometric mode (i.e. fixing the stack voltage) but may be more delicate while in chronopotentiometric operation (i.e. fixing the current), whenever the substrate is not correctly distributed/replaced within the individual MECs of the stack. The power efficiency of the CBS is strictly linked with the diodes (or line of diodes) selected for the bypass line, and the applied stack voltage. By correctly setting-up these two parameters, it is possible to reach high power efficiencies, comparable with those of active control systems. The developed CBS can be applied to different BES technologies, allowing to increase their voltage requirements, and facilitating their industrial uptake.

Funding

This work has been financially supported by the Spanish Ministry of Economy and Competitiveness, under the project Power2Biomethane (RTC-2016-5024-3, 2016), and by the European Union's Horizon 2020 Research and Innovation programme, under the project GREENER (Grant Agreement Nº 826312).

CRediT authorship contribution statement

Daniele Molognoni: Conceptualization, Methodology, Investigation, Writing - original draft. **Pau Bosch-Jimenez:** Conceptualization, Methodology, Investigation, Writing - review & editing. **Jordi Suarez:** Conceptualization, Methodology, Writing - review & editing. **Monica Della Pirriera:** Conceptualization, Writing - review & editing, Supervision, Project administration. **Eduard Borràs:** Conceptualization, Writing - review & editing, Supervision, Project administration.

Declaration of competing interest

The authors declare that they have no known competing financial interests or personal relationships that could have appeared to influence the work reported in this paper.

Acknowledgements

The authors wish to acknowledge the other Leitat collaborators who took part in the Power2Biomethane and GREENER projects.

Appendix A. Supplementary data

Supplementary data to this article can be found online at https://doi.org/10.1016/j.jpowsour.2021.229576.

Glossary

BES	Bioelectrochemical system
CBS	Cell balance system
COD	Chemical oxygen demand
CV	Cyclic voltammetry
MEC	Microbial electrolysis cell
MES	Microbial electrosynthesis (cell)
MFC	Microbial fuel cell
MMO	Mixed metal oxide

References

[1] K. Rabaey, R.A. Rozendal, Microbial electrosynthesis - revisiting the electrical route for microbial production, Nat. Rev. Microbiol. 8 (2010) 706–716.
[2] F. Harnisch, F. Aulenta, U. Schröder, in: second ed.Microbial Fuel Cells and Bioelectrochemical Systems. Comprehensive Biotechnology, 1, Elsevier, 2011, pp. 643–659.
[3] A.P. Borole, G. Reguera, B. Ringeisen, Z.-W. Wang, Y. Feng, B.H. Kim, Electroactive biofilms: current status and future research needs, Energy Environ. Sci. 4 (2011) 4813.
[4] R. Rodríguez-Alegre, A. Ceballos-Escalera, D. Molognoni, P. Bosch-Jimenez, D. Galí, E. Licon, et al., Integration of membrane contactors and bioelectrochemical systems for CO_2 conversion to CH_4, Energies 12 (2019) 361, 361.
[5] H. Wang, Z.J. Ren, A comprehensive review of microbial electrochemical systems as a platform technology, Biotechnol. Adv. 31 (2013) 1796–1807.
[6] U. Schröder, F. Harnisch, L.T. Angenent, Microbial electrochemistry and technology: terminology and classification, Energy Environ. Sci. 8 (2015) 513–519.
[7] A. Ceballos-Escalera, D. Molognoni, P. Bosch-Jimenez, M. Shahparasti, S. Bouchakour, A. Luna, et al., Bioelectrochemical systems for energy storage: a scaled-up power-to-gas approach, Appl. Energy 260 (2020) 114138.
[8] M. Ramírez-Moreno, P. Rodenas, M. Aliaguilla, P. Bosch-Jimenez, E. Borràs, P. Zamora, et al., Comparative performance of microbial desalination cells using air diffusion and liquid cathode reactions: study of the salt removal and desalination efficiency, Front Energy Res 7 (2019) 135.
[9] N. Pous, M.D. Balaguer, J. Colprim, S. Puig, Opportunities for groundwater microbial electro-remediation, Microb Biotechnol 11 (2018) 119–135.

[10] Z. Dou, C.M. Dykstra, S.G. Pavlostathis, Bioelectrochemically assisted anaerobic digestion system for biogas upgrading and enhanced methane production, Sci. Total Environ. 633 (2018) 1012–1021.
[11] A. Escapa, M.I. San-Martín, R. Mateos, A. Morán, Scaling-up of membraneless microbial electrolysis cells (MECs) for domestic wastewater treatment: bottlenecks and limitations, Bioresour. Technol. 180 (2015) 72–78.
[12] R. Rousseau, L. Etcheverry, E. Roubaud, R. Basséguy, M.-L. Délia, A. Bergel, Microbial electrolysis cell (MEC): strengths, weaknesses and research needs from electrochemical engineering standpoint, Appl. Energy 257 (2020) 113938.
[13] E.S. Heidrich, J. Dolfing, K. Scott, S.R. Edwards, C. Jones, T.P. Curtis, Production of hydrogen from domestic wastewater in a pilot-scale microbial electrolysis cell, Appl. Microbiol. Biotechnol. 97 (2013) 6979–6989.
[14] F. Enzmann, D. Holtmann, Rational Scale-Up of a methane producing bioelectrochemical reactor to 50 L pilot scale, Chem. Eng. Sci. 207 (2019) 1148–1158.
[15] X.A. Walter, I. Merino-Jiménez, J. Greenman, I. Ieropoulos, PEE POWER®urinal II – urinal scale-up with microbial fuel cell scale-down for improved lighting, J. Power Sources 392 (2018) 150–158.
[16] C.J. Castro, J.E. Goodwill, B. Rogers, M. Henderson, C.S. Butler, Deployment of the microbial fuel cell latrine in Ghana for decentralized sanitation, J. Water, Sanit. Hyg. Dev. 4 (2014) 663–671.
[17] P. Aelterman, K. Rabaey, H.T. Pham, N. Boon, W. Verstraete, Continuous electricity generation at high voltages and currents using stacked microbial fuel cells, Environ. Sci. Technol. 40 (2006) 3388–3394.
[18] J. Choi, Y. Ahn, Continuous electricity generation in stacked air cathode microbial fuel cell treating domestic wastewater, J. Environ. Manag. 130 (2013) 146–152.
[19] P Dessì, L Rovira-Alsina, C. Sánchez, G.K. Dinesh, W. Tong, et al., Microbial electrosynthesis: towards sustainable biorefineries for production of green chemicals from CO_2 emissions, Biotechnol. Adv. (2020), 107675, https://doi.org/10.1016/j.biotechadv.2020.107675.
[20] B.E. Logan, B. Hamelers, R. Rozendal, U. Schröder, J. Keller, S. Freguia, et al., Microbial fuel cells: Methodology and technology, Environ. Sci. Technol. 40 (2006) 5181–5192.
[21] S.J. Andersen, I. Pikaar, S. Freguia, B.C. Lovell, K. Rabaey, R a Rozendal, Dynamically adaptive control system for bioanodes in serially stacked bioelectrochemical systems, Environ. Sci. Technol. 47 (2013) 5488–5494.
[22] R. Muñoz-Aguilar, D. Molognoni, P. Bosch-Jimenez, E. Borràs, M. Della Pirriera, Á. Luna, Design, operation, modeling and grid integration of power-to-gas bioelectrochemical systems, Energies 11 (2018) 1947, 1947.
[23] P.K. Wu, J.C. Biffinger, L.A. Fitzgerald, B.R. Ringeisen, A low power DC/DC booster circuit designed for microbial fuel cells, Process Biochem. 47 (2012) 1620–1626.
[24] H. Wang, J. Park, Z.J. Ren, Practical energy harvesting for microbial fuel cells: a review, Environ. Sci. Technol. 49 (2015) 3267–3277.
[25] X. Chen, F.L. Lobo, Y. Bian, L. Lu, X. Chen, M.P. Tucker, et al., Electrical decoupling of microbial electrochemical reactions enables spontaneous H_2 evolution, Energy Environ. Sci. 13 (2020) 495–502.
[26] S.E. Oh, B.E. Logan, Voltage reversal during microbial fuel cell stack operation, J. Power Sources 167 (2007) 11–17.
[27] J. An, H.-S. Lee, Occurrence and implications of voltage reversal in stacked microbial fuel cells, ChemSusChem 7 (2014) 1689–1695.
[28] B. Kim, S.V. Mohan, D. Fapyane, I.S. Chang, Controlling voltage reversal in microbial fuel cells, Trends Biotechnol. 38 (6) (2020) 667–678.
[29] J. An, J. Sim, H.S. Lee, Control of voltage reversal in serially stacked microbial fuel cells through manipulating current: significance of critical current density, J. Power Sources 283 (2015) 19–23.
[30] B. Kim, B.-G. Lee, B.H. Kim, I.S. Chang, Assistance current effect for prevention of voltage reversal in stacked microbial fuel cell systems, CHEMELECTROCHEM 2 (2015) 755–760.
[31] B. Kim, I.S. Chang, Elimination of voltage reversal in multiple membrane electrode assembly installed microbial fuel cells (mMEA-MFCs) stacking system by resistor control, Bioresour. Technol. (2018) 1.
[32] G. Papaharalabos, A. Stinchcombe, I. Horsfield, C. Melhuish, J. Greenman, I. Ieropoulos, Autonomous energy harvesting and prevention of cell reversal in MFC stacks, J. Electrochem. Soc. 164 (2017) H3047–H3051.
[33] Y. Kim, M.C. Hatzell, A.J. Hutchinson, B.E. Logan, Capturing power at higher voltages from arrays of microbial fuel cells without voltage reversal, Energy Environ. Sci. 4 (2011) 4662, 4662.
[34] N.H. Kutkut, D.M. Divan, Dynamic equalization techniques for series battery stacks, in: Proceedings of Intelec'96 - International Telecommunications Energy Conference, IEEE, Boston, MA, USA, 1996, pp. 514–521.
[35] R. Rossi, B.E. Logan, Unraveling the contributions of internal resistance components in two-chamber microbial fuel cells using the electrode potential slope analysis, Electrochim. Acta 348 (2020) 136291.
[36] X. Yang, Y. Li, L. Deng, W. Li, Z. Ren, M. Yang, et al., Synthesis and characterization of an IrO2–Fe2O3 electrocatalyst for the hydrogen evolution reaction in acidic water electrolysis, RSC Adv. 7 (2017) 20252–20258.
[37] F. Zhang, J. Liu, I. Ivanov, M.C. Hatzell, W. Yang, Y. Ahn, et al., Reference and counter electrode positions affect electrochemical characterization of bioanodes in different bioelectrochemical systems, Biotechnol. Bioeng. 9999 (2014) 1–9.
[38] P. Bosch-Jimenez, S. Martinez-Crespiera, D. Amantia, M.D. Pirriera, I. Forns, R. Shechter, et al., Non-precious metal doped carbon nanofiber air-cathode for Microbial Fuel Cells application: oxygen reduction reaction characterization and long-term validation, Electrochim. Acta 228 (2017) 380–388.
[39] M. Miskan, M. Ismail, M. Ghasemi, J. Md Jahim, D. Nordin, M.H. Abu Bakar, Characterization of membrane biofouling and its effect on the performance of microbial fuel cell, Int. J. Hydrogen Energy 41 (2016) 543–552.